Paulcy Rani Palayyan Raja Bai[1], Sivakala Sarojam[2], Anju Krishna Salimkumar Shailaja[1], Anu Mini Aravind[3], Xavier Thankappan Suryabai[3]

[1] Department of Chemistry, Government College for Women, Thiruvananthapuram 14, Kerala; [2] Department of Chemistry, Sree Narayana College, Chempazhanthy, Thiruvananthapuram, Kerala; [3] Centre for advanced materials research, Department of Physics, Government College for Women, Thiruvananthapuram 14, Kerala

Scientific Paper
ISSN 0351-9465, E-ISSN 2466-2585
https://doi.org/10.62638/ZasMat1175

Zastita Materijala 65 (4)
778 – 785 (2024)

The Electrochemical Performance of Perovskite $LaMnO_3$

ABSTRACT

Perovskite oxides have attracted as promising electrode materials for supercapacitors because of their unique structure, compositional flexibility, and inherent oxygen vacancy. In the present work, $LaMnO_3$(LMO) perovskites are synthesised by microwave assisted chemical coprecipitation and followed by calcination at 750 ˚C. The crystal structure and the presence of functional groups in $LaMnO_3$ were studied through X-ray diffraction (XRD) and Fourier transform infrared spectroscopy (FT-IR). The surface morphology was characterized by field emission scanning electron microscopy (FESEM). Electrochemical performance of LMO electrodes is evaluated in 3M KOH and 3M NaOH electrolytes. The specific capacitance of the LMO electrode in 3M NaOH and 3M KOH electrolyte were calculated to be 557.76F/g and 290.63F/g at scan rate of 5mV/s. The enhancement in the specific capacitance of the LMO electrode in 3M NaOH can be attributed to the effective charge storage mechanism.

Keywords: *Microwave, $LaMnO_3$ perovskite, electrochemical performance, specific capacitance*

1. INTRODUCTION

Constantly increasing energy demands and environmental pollution have compelled us to seek environment friendly and renewable energy resources. Energy-storage technologies such as batteries, supercapacitors, and fuel cells are important for sustaining renewable energy resources [1]. Electrochemical supercapacitors gain prime importance as electrochemical energy storage due to their high-power densities at reasonably high energy densities and significantly long cycle life so that they can be used in heavy electric vehicles and consumer electronic devices, industrial power management, and military devices [2-4]. Supercapacitor is a device that have higher specific capacitance and minimum internal resistance, which is composed of two electrodes separated by a separator and an electrolyte. The performance of a supercapacitor mainly depends upon the selection of the electrode material. Based on the charge storage mechanism, SCs can be classified into two categories as electrochemical double layer capacitors (EDLCs) and pseudo capacitors (PCs) [5]. EDLCs store charge through charge accumulation at the interface between the electrolyte and the electrode's surface. EDLCs store charge through non faradic process in which charge separation and accumulation take place at the active material and electrolyte interface. Because of their high specific surface area and desirable conductivity, carbon-based materials such as carbon nanotubes, activated carbon, graphene, graphene oxide and reduced graphene oxide are the most attractive active material for EDLCs [6,7]. Where as in pseudo capacitance type of mechanism the oxidation and reduction reactions take place between electrode and electrolyte that results in the charge transportation. Since the electrochemical reactions occur both on the surface and in the bulk near the solid electrode surface, PCs often show far higher capacitance values and energy densities than EDLCs [8]. Conducting Polymers and transition metal oxides such as MnO_2, NiO, $Fe_2O_3$and Co_3O_4 can act as electrode material for pseudo capacitors.

Perovskite oxides with ABO_3 formula have been widely investigated for their applications in catalysis [9], water splitting [10], supercapacitance [11], bat-

* Corresponding author: Paulcy Rani P R
E-mail: pr.paulcyrani@gmail.com
Paper received: 22.04.2024.
Paper accepted: 20.05.2024.

teries [12], optical [13], superconductivity [14], etc., and are considered to be a replacement for single oxides in the stipulated application. The ABO_3 perovskites are promising for supercapacitance owing to the presence of multiple transition- metal ions in their crystal structure and therefore, perovskite oxides have the potential to enhance the performance of the supercapacitor through different charge storing mechanisms [15,16], by controlling the ratio of metallic ions used during the synthesis [17]. Moreover, perovskite oxides are capable of accommodating a large number of inherent oxygen vacancies [18].

In the present work, perovskite nano $LaMnO_3$(LMO) was prepared by microwave assisted co-precipitation. The electrochemical performance of the LMO electrodes is examined in electrolytes such as 3M KOH and 3M NaOH.

2. EXPERIMENTAL DETAILS

$LaMnO_3$ perovskites were synthesised by microwave assisted chemical coprecipitation. A mixture of 0.5 molar solutions Lanthanum (III)chloride and Manganese (II)chloride in the molar ratio of 1:1 is taken and stirred in a magnetic stirrer. Then1M NaOH is added to the solution with stirring and then heated in a microwave oven for 10 minutes. Finally, the precipitate was filtered, washed with distilled water, dried in air oven at 80ºC for 24 hours and calcinated in a muffle furnace at 750 ˚C for 12 h at a heating rate 2ºC per minute.

2.2 Characterizations

The functional groups present in the material are analysed using FT-IR spectroscopy, performed in Perkin-Elmer 'Spectrum Two' FT-IR Spectrometer. The structural properties of the material are analysed by X-ray diffraction (XRD) Rigaku Miniflex-600 benchtop diffractometer with a Cu Kα radiation source (λ = 1.542 Å) in the range 10−90°. The morphology of the sample was analysed using FESEM with EDX (CARL ZEISS USA, resolution 1.5nm). BET(Brunauer-Emmett-Teller) analysis (Altamira Instruments, Inc) was carried out to examine surface area and pore size distribution using nitrogen adsorption-desorption isotherms. All Electrochemical investigations were carried out in BioLogic VSP electrochemical workstation with three electrode system. Nickel foam casted with an active electrode material act as working electrode, Platinum wire acts counter electrode and Ag/AgCl electrode act as reference electrode.

2.3 Preparation of working electrode and electrochemical study

Before the preparation of electrode, the Ni-foam (1 cm X 1 cm) was cleaned with detergent, ethanol, concentrated hydrochloric acid and washed several times with DI water to eliminate the impurities and surface oxidant contents. To prepare the working electrodes, the electrode material (80%), polyvinylidene fluoride binder (10%) and carbon black (10%) were first mixed together using a mortar-pestle to make slurry using N-methyl-2-pyrrolidinone solvent. This slurry was drop casted into Ni-foam (1 cm X 1 cm) and dried at 120°C for 5h. The prepared electrodes were used for electrochemical characterizations.

The electrochemical performance of the prepared electrode material was tested through CV techniques. The electrochemical tests are performed in BioLogic VSP electrochemical workstation with three electrode system. Nickel foam casted with an active electrode material, Platinum wire and Ag/AgCl electrode are used as working, counter and reference electrodes respectively. The CV measurements were carried over a potential range of -0.4 to 0.6V at scan rate from 5 mV/s to 100 mV/s. Various aqueous electrolytes such as 3M NaOH and 3M KOH were used in the electrochemical measurements.

3 RESULTS AND DISCUSSION

3.1 FT-IR

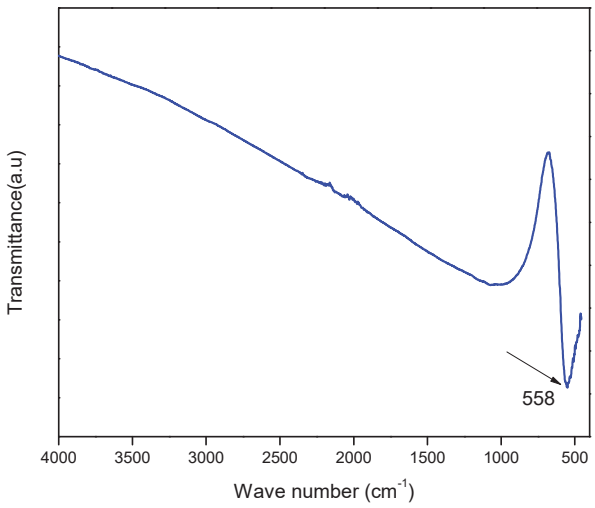

Fig. 1 FT IR Spectrum of LMO

FTIR analysis is performed to study the vibrational spectrum of perovskite $LaMnO_3$ as shown in Fig.1. The strong absorption peak at 558 cm^{-1} is corresponding to Mn-O vibrations. The presence of this vibrational peak is the characteristic of the ABO_3 type perovskite which confirms the successful synthesis of perovskite $LaMnO_3$[19].

3.2 XRD Analysis

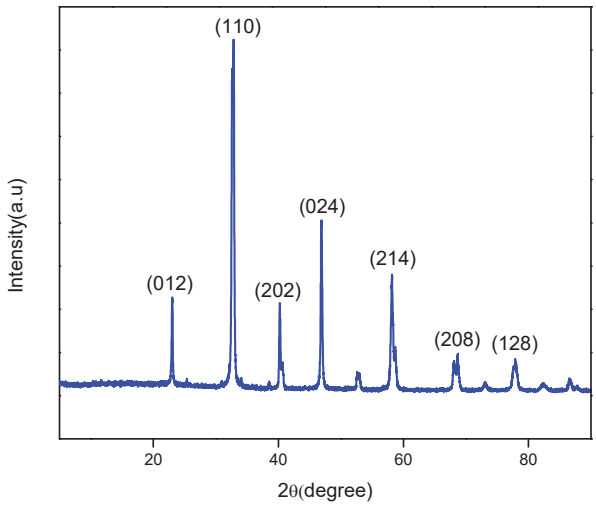

Fig. 2. XRD pattern of LMO

The XRD pattern of the synthesised compound is well matched with JCPDS 89-8775, which corresponds to rhombohedral perovskite structure of $LaMnO_3$ with R-3c group. The peaks at 2θ values 23.2˚, 32.9˚, 40.3˚, ˚46.86˚, 58.3˚, 68.6˚and 78.05˚ are corresponding to (012), (110), (202), (024), (214), (208), (128) planes. The strongest diffraction peak occurs at 2θ value 32.7˚ which is the characteristic diffraction peak of $LaMnO_3$. The highly crystalline nature of the synthesised material is confirmed by the narrow and strong diffraction peaks.

3.3 Brunauer-Emmett-Teller (BET) surface area analysis

The surface area of the synthesised LMO is analysed by N2 adsorption-desorption at 77K. The nitrogen adsorption-desorption isotherm for LMO is displayed in Fig 3. (a). From the BET analysis surface area was evaluated to be 2.703m^2g^{-1}. The BJH (Barrett, Joyner, and Halenda) pore size distribution diagrams of LMO electrode material are displayed in figure 3. (b). From the figure it is examined that the material shows broad distribution curves. The average pore diameter of LMO was evaluated as 9.027nm in the mesoporous region of LMO. The mesoporous nature of the electrode material determines charge transport across the electrode-electrolyte interface.

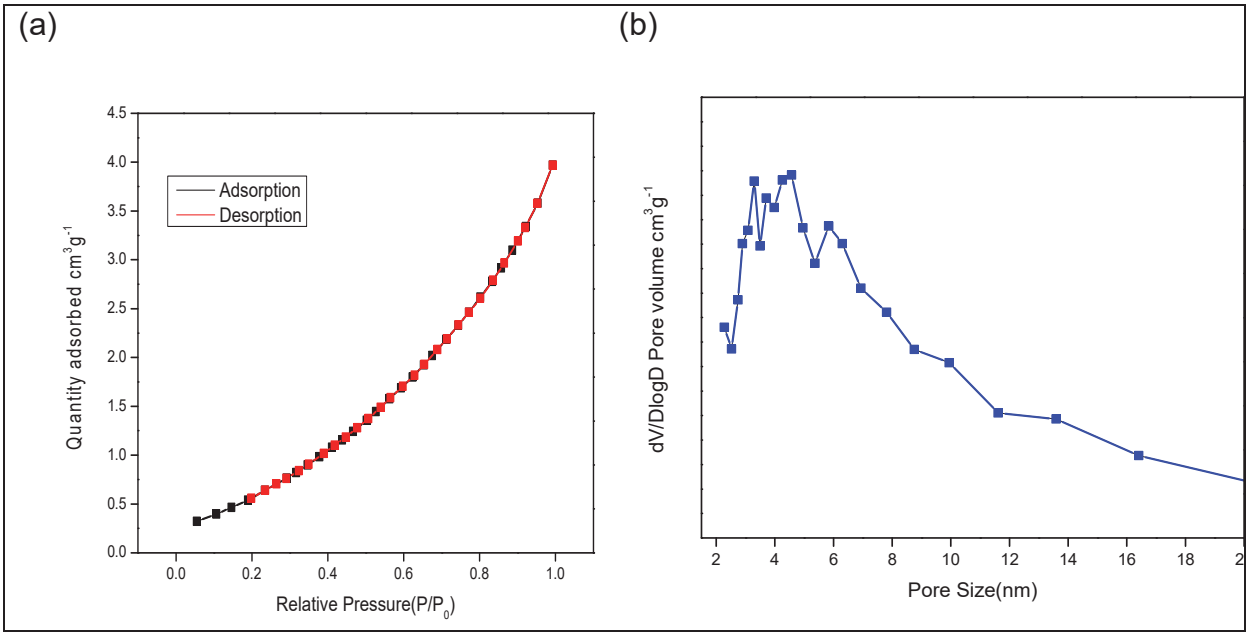

Fig 3 (a) BET Nitrogen adsorption-desorption isotherms of LMO
(b) Pore size distribution curve of LMO.

3.4 Morphological study

Surface morphology of the prepared material is examined through FESEM analysis, micrograph demonstrate there is agglomeration of nano particles and reveals the presence three-dimensional nano crystalline nature of the material. (Figure 4.). The X-ray energy dispersive spectrum (EDAX) (Fig. 4(d)) shows that La, Mn and O elements are in a molar ratio of 1: 1: 3 in the synthesised material, which confirms that the obtained product is $LaMnO_3$.

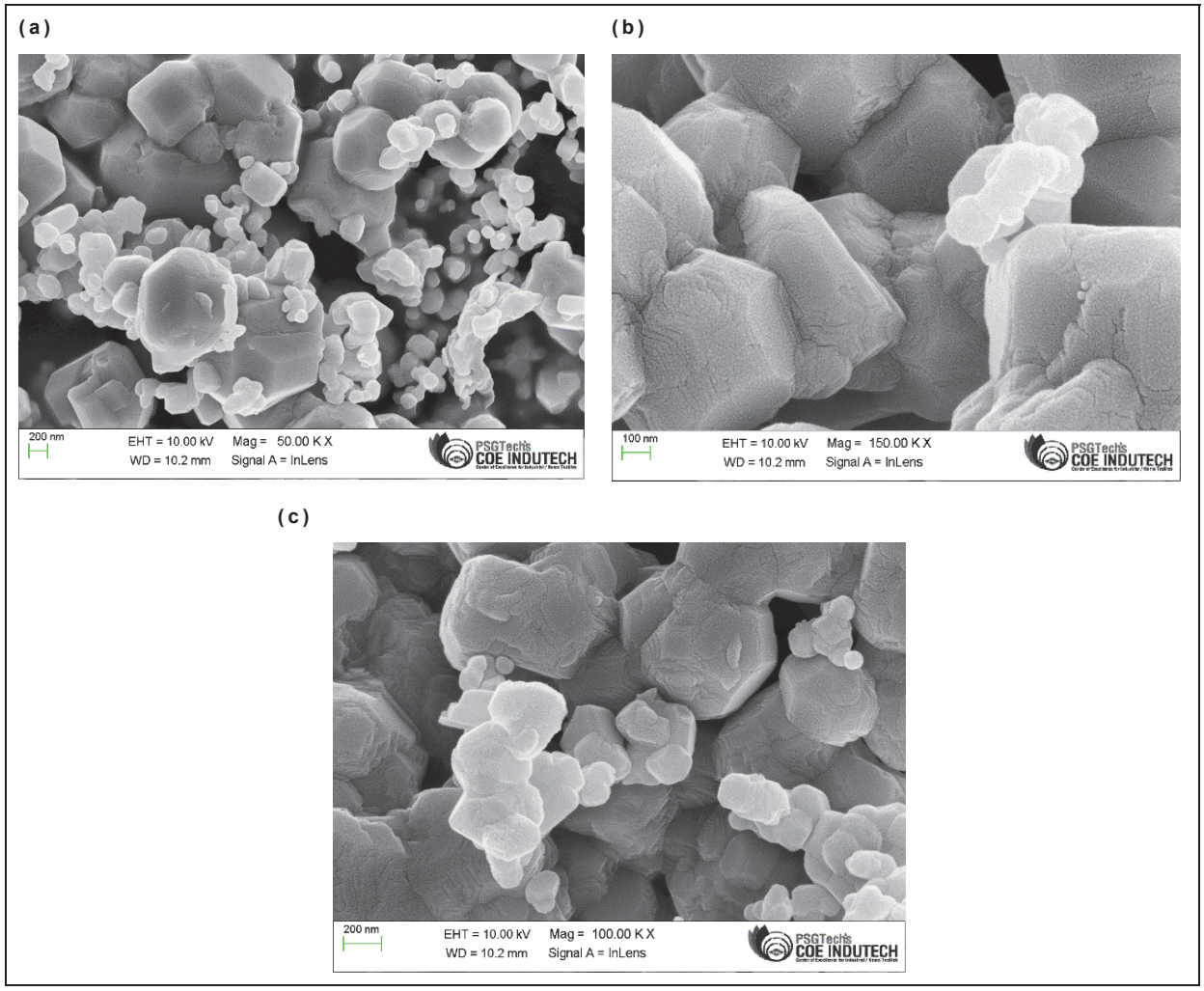

Fig 4. FE-SEM micrographs of the LMO at different magnification(a) (b)and (c)

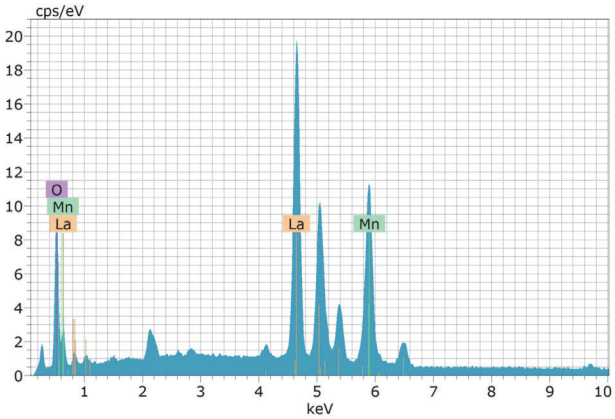

Fig.4(d) EDAX spectrum of LMO.

3.5 Electrochemical study

The electrochemical performances of the synthesised LMO material as electrode materials for supercapacitors were examined by Cyclic voltammetry (CV), and Electrochemical impedance spectroscopy (EIS). The electrochemical tests are performed in BioLogic VSP electrochemical workstation with three electrode system. Nickel foam casted with an active electrode material, platinum wire and Ag/AgCl electrode are used as working, counter and reference electrodes respectively. The CV measurements were carried over a potential range of -0.4 to 0.6V in aqueous electrolytes such as 3M KOH and 3M NaOH at scan rate from 5 mV/s to 100 mV/s. EIS measurement was carried over wide frequency range of 200KHz to 100mHz applying an AC voltage of 1 mV.

3.5.1 Cyclic voltammetry (CV)

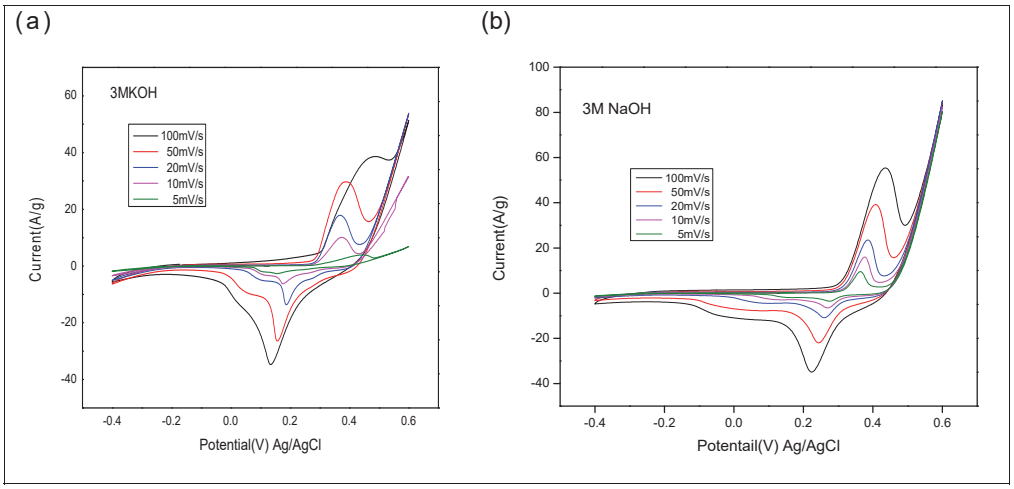

Fig.5. CV plot of LMO in (a)3MKOH and (b)3MNaOH electrolyte.

The electrochemical performance of the as-prepared LMO electrode was analysed by cyclic voltammetry in 3M KOH and 3M NaOH electrolytes at different scan rates, as shown in Fig. 5. The redox peaks are clearly observed in the CV curve for both the electrolytes, this confirms the pseudocapacitive nature of the LMO electrodes. These redox peaks are mainly due to the fast reversible process of ionic intercalations on the electrode material. The change in oxidation state of manganese as $Mn^{+2} \leftrightarrow Mn^{+3}$ and $Mn^{+3} \leftrightarrow Mn^{+4}$ favours the ionic intercalation/deintercalation in the electrode material.

The Specific capacitance of LMO electrodes is calculated by Equation (1)

$$C_s = \frac{\int_{v1}^{v2} i(v)dv}{(v2 - v1)ms} \quad (1)$$

where the numerator indicated the total charge enclosed by the CV curve, (v2 -v1) is the working potential window, m is the mass, and sis the scan rate. The area under the CV curve is directly proportional to the specific capacitance of the electrode material. The specific capacitance of the LMO electrodes in 3 M KOH electrolyte is determined as 290.63, 184.76, 157.14, 84.33 and 52.19 F/g for 5, 10, 20, 50 and 100 mV/s. LMO electrodes have achieved higher specific capacitance at lower scan rate. This is because at lower scan rate, the electrolyte ions get access to the entire active sites of the electrode material. However, at the higher scan rates, the electrolyte ions get insufficient time for diffusion [20].

From CV curve it is appeared that area of the CV curve of the LMO electrode in 3 M NaOH is larger than that of 3 M KOH. Table:1 summarizes the specific capacitance values of the LMO electrode material determined from the CV plots at different scan rates in3M KOH and 3M NaOH electrolyte. The specific capacitance of the LMO electrode in 3M NaOH and 3M KOH electrolyte were found to be 557.76F/g and 290.63F/g at scan rate of 5mV/s. This is enhanced electrochemical performance in NaOH is due to the increased ionic mobility and diffusivity of Na^+ ions are compared the K^+ ions, that leads to better diffusion of Na^+ and thus facilitates the fast charge transport across the electrolyte–electrode interface. Therefore, LMO electrodes exhibit better electrochemical performance in NaOH than KOH electrolyte [21].

Table1. The specific capacitance values of the LMO electrode material calculated from the CV plots at different scan rates in 3M KOH and 3M NaOH electrolyte.

Scan rate(mV/s)	Specific Capacitance F/g	
	3M KOH	3M NaOH
5	290.63	557.76
10	184.76	317.38
20	157.14	190.00
50	84.33	97.67
100	52.19	65.02

3.5.2 Electrochemical impedance spectroscopy (EIS)

EIS study has been performed for analysing resistance that occurs due to charge transportation and diffusion of active material. The Nyquist plot for LMO electrodes obtained in 3M KOH and 3M NaOH are shown in Fig.6. This EIS spectrum shows straight line in lower frequency and a semi-circle in high frequency. The internal resistance (Rs) of the cell consists of intrinsic resistance of the electrode material, contact resistance between current collector and electrode, and resistance offered by an electrolyte. Rct is the charge transfer resistance resulting from the faradic reactions at the electrode–electrolyte boundary [22]. The internal resistance and charge transfer resistance are calculated by using Zfit of the EC lab software. The values of Rs and Rct determined from EIS analysis are 0.97Ω and 2.50Ω in 3M KOH, 0.67 Ω and 0.86Ω in 3M NaOH electrolyte. The lower values of Rs and Rct is obtained for electrode material in 3M NaOH and LMO electrodes exhibit enhanced electrochemical performance in 3M NaOH over 3M KOH.

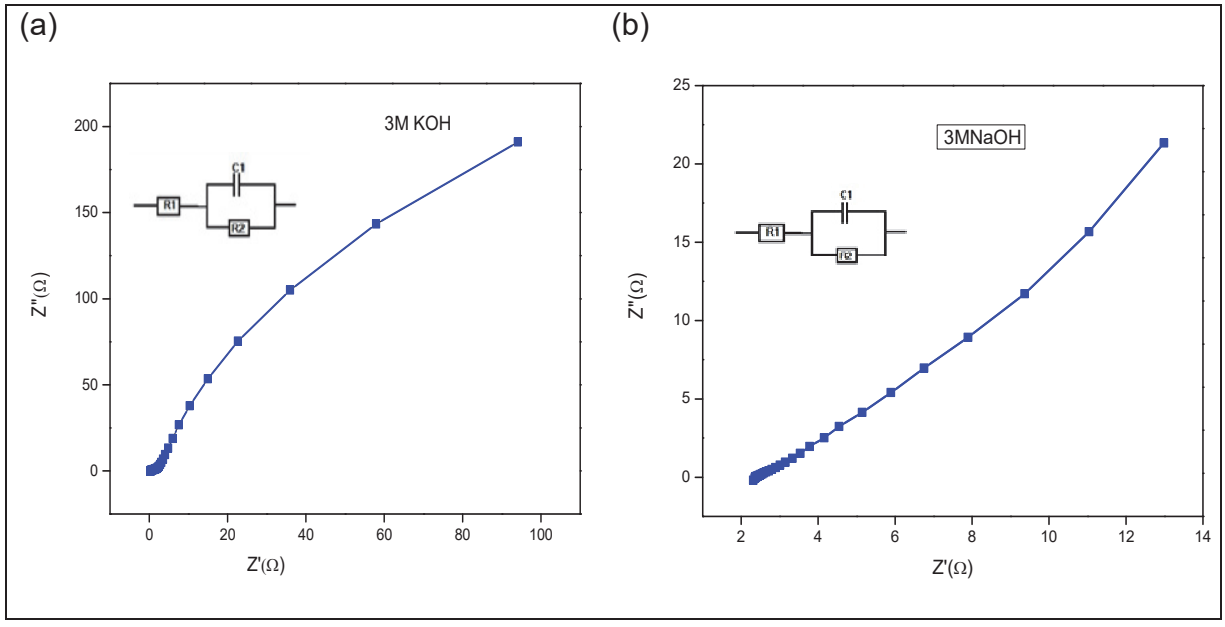

Fig.6 EIS plot of LMO(a) 3M KOH and (b) 3M NaOH

4 CONCLUSIONS

Perovskite $LaMnO_3$ nanoparticles was successfully synthesized by facile microwave assisted co-precipitation. The XRD analysis confirms the highly crystalline nature of the synthesised perovskite $LaMnO_3$ by the narrow and strong diffraction peaks. The mesoporous nature of the LMO electrode material was confirmed through BET analysis with a specific surface area of 2.703$m^2g^{-1}$and an average pore diameter of 9.08nm. The specific capacitance of the LMO electrode in 3M NaOH and 3M KOH electrolyte was found to be 557.76F/g and 290.63F/g at scan rate of 5mV/s. Therefore, LMO electrodes exhibit better electrochemical performance in NaOH than KOH electrolyte. The lower values of Rs and Rct is obtained for electrode material in 3M NaOH and LMO electrodes exhibit enhanced electrochemical performance in 3M NaOH. These results suggest that the perovskite $LaMnO_3$ electrode material are prominent candidates for fabricating efficient electrochemical capacitors.

Acknowledgements

For analytical support, the authors acknowledge the Centralized Common Instrumentation Facility (CCIF), Government College for Women, Thiruvananthapuram.

REFERENCES

[1] Zh. Sanliang, Y. Li, N. Pan (2012) Graphene based supercapacitor fabricated by vacuum filtration deposition, Journal of Power Sources., 206, 476–482. doi.10.1016/j.jpowsour.2012.01.124.

[2] S. Zheng, H. Xue, H. Pang (2018) Supercapacitors based on metal coordination materials, Co-ordination chemistry Reviews., 373, 2–21. doi.org/10.1016/j.ccr.2017.07.002.

[3] Y.Yang, D.Cheng, S.Chen, Y.Guan, J.Xiong (2016) Construction of hierarchical $NiCo_2S_4$@Ni $(OH)_2$ core-shell hybrid nanosheet arrays on Ni foam for high-performance aqueous hybrid supercapacitors, Electrochimica Acta., 193,116–127. doi: 10.1016/j.electacta.2016.02.053.

[4] S.Bose, T.Kuila, A.Mishra, R.Rajasekar N.Kim, J.Lee (2012) Carbon-based nanostructured materials and their composites as supercapacitor electrodes, Journal Materials Chemistry., 22, 767–784. doi. 10.1039/c1jm14468e.

[5] J. Yan, S.i Li, B. Lan, Y. Wu (2019) Rational design of nanostructured electrode materials toward multifunctional supercapacitors, Advanced functional materials reviews.,1902564, 1-35. doi.10.1002/adfm.201902564.

[6] L.Candelaria, L.Stephanie, Y.Shao, W.Zhou, X. Li, J. Xiao, J. Guang Zhang, Y. Wang, J. Liu, J. Li, G. Cao (2012) Nanostructured carbon for energy storage and conversion, Nano Energy., 1,195–220. Doi.10.1016/j.nanoen.2011.11.006.

[7] Y. Wang, L. Zhang, H. Hou, W. Xu, G. Duan, S. He, K. Liu, S. Jiang (2021) Recent progress in carbon-based materials for supercapacitor electrodes: a review, Journal of Material Science., 56, 173–200. doi.10.1007/s10853-020-05157-6.

[8] Y. Liu, Z. Wang, Y. Zhong, X. Xu, J.-P. M. Veder, M. R. Rowles, M. Saunders, R. Ran, Z Shao (2020) Activation-free supercapacitor electrode based on surface-modified $Sr_2CoMo_{1-x}Ni_xO_{6-\delta}$ perovskite, Chemical Engineering Journal., 390, 124645, 1-10. doi.org/10.1016/j.cej.2020.124645.

[9] A.H. McDaniel, A. Ambrosini, E.N. Coker, J.E. Miller, W.C. Chueh, R. O Hayre, J. Tong (2014) Nonstoichiometric perovskite oxides for solar thermochemical H_2 and CO production, Energy Procedia., 49, 2009–2018. doi.org/10.1016/j.egypro.2014.03.213

[10] J. Wang, Y. Gao, D. Chen, J. Liu, Z. Zhang, Z. Shao, F. Ciucci (2017) Water splitting with an enhanced bifunctional double perovskite, ACS Catalysis., 8, 1, 364–371. doi.org/10.1021/acscatal.7b02650.

[11] Y. Liu, J. Dinh, M.O. Tade, Z. Shao (2016) Design of perovskite oxides as anion-intercalation-type electrodes for supercapacitors: cation leaching effect, ACS Applied Materials and Interfaces., 8(36), 23774–23783. doi.org/10.1021/acsami.6b08634.

[12] P. Tan, M. Liu, Z. Shao (2017) Recent advances in perovskite oxides as electrode materials for nonaqueous lithium–oxygen batteries, Advanced Energy Materials., 7, 1602674,1-23. doi.10.1002/aenm.201602674.

[13] Y. Yamada, Y. Kanemitsu (2013) Photoluminescence spectra of perovskite oxide semiconductors, Journal of Luminescence., 133, 30–34, doi: 10.1016/j.jlumin.2011.12.037.

[14] C.N.R.Rao (1990) Perovskite oxides and high-temperature superconductivity, Ferroelectrics.,102, 297–308. Doi.10.1080/00150199008221489.

[15] N. Arjun, G.-T. Pan, T.C.K. Yang (2017) The exploration of lanthanum-based perovskites and their complementary electrolytes for the supercapacitor applications, Results in Physics., 7, 920–926. doi.org/10.1016/j.rinp.2017.02.013.

[16] J.T. Mefford, W.G. Hardin, S. Dai, K.P. Johnston, K. J.Stevenson (2014) Anion charge storage through oxygen intercalation in $LaMnO_3$ perovskite pseudo capacitor electrodes, Nature Materials., 13, 726–732. doi.10.1038/NMAT4000.

[17] J. Zhu, H. Li, L. Zhong, P. Xiao, X. Xu, X. Yang, Z. Zhao, J. Li (2014) Perovskite oxides: preparation, characterizations, and applications in heterogeneous catalysis, ACS Catalysis., 4, 2917–2940. doi.org/10.1021/cs500606g.

[18] F. Galasso (1990) Perovskites and High Tc Superconductors Routledge, New York.

[19] J.Hu, J.Ma, L.Wang, H.Huang, L.Ma (2014) Preparation, characterization and photocatalytic activity of co-doped $LaMnO_3$/graphene composites, Powder Technology., 254, 556-562. doi.org/10.1016/j.powtec.2014.01.071.

[20] N. Maheswari, G. Muralidharan (2015) Supercapacitor behaviour of cerium oxide nanoparticles in neutral aqueous electrolytes, Energy and Fuels., 29(12), 8246–8253. doi. 10.1021/acs.energyfuels.5b02144.

[21] D.Lundberg, D.Warmińska, A.Fuchs, I. Persson (2018) On the relationship between the structural and volumetric properties of solvated metal ions in O-donor solvents using new structural data in amide solvents, Physical Chemistry Chemical Physics., **20**, 14525-14536. Doi.10.1039/x0xx00000x.

[22] P. Gao, P. Metz, T. Hey, Y. Gong, D. Liu, D.D. Edwards, J.Y. Howe, R. Huang, S. T. Misture (2017) The critical role of point defects in improving the specific capacitance of δ-MnO_2 nanosheets, Nature Communications., 8,14559. doi: 10.1038/ncomms14559.

IZVOD

ELEKTROHEMIJSKE PERFORMANSE PEROVSKITA LAMNO3

Perovskit oksidi su se privukli kao obećavajući elektrodni materijali za superkondenzatore zbog svoje jedinstvene strukture, fleksibilnosti kompozicije i inherentne praznine za kiseonik. U ovom radu, $LaMnO_3$(LMO) perovskiti se sintetišu hemijskom koprecipitacijom uz pomoć mikrotalasne pećnice, a zatim kalcinacijom na 750 ˚C. Kristalna struktura i prisustvo funkcionalnih grupa u $LaMnO_3$ proučavani su difrakcijom rendgenskih zraka (XRD) i infracrvenom spektroskopijom Furijeove transformacije (FT-IR). Morfologija površine je okarakterisana pomoću polja emisione skenirajuće elektronske mikroskopije (FESEM). Elektrohemijske performanse LMO elektroda se procenjuju u 3M KOH i 3M NaOH elektrolitima. Specifični kapacitet LMO elektrode u 3M NaOH i 3M KOH elektrolitu je izračunat na 557,76F/g i 290,63F/g pri brzini skeniranja od 5mV/s. Povećanje specifične kapacitivnosti LMO elektrode u 3M NaOH može se pripisati efikasnom mehanizmu skladištenja naelektrisanja.

Ključne reči: *mikrotalasna pećnica, LaMnO3, perovskit, elektrohemijske performanse, specifična kapacitivnost*

ORCID Numbers of all the authors

Paulcy Rani Palayyan Raja Bai: https://orcid.org/0009-0003-4200-1474

Anju Krishna Salimkumar Shailaja: https://orcid.org/0009-0005-1453-3021

Sivakala Sarojam: https://orcid.org/0000-0002-2126-1790

Anu Mini Aravind: https://orcid.org/0000-0002-2941-208X

Xavier Thankappan Suryabai: https://orcid.org/0000-0001-8955-0743

Naučni rad

Rad primljen 23.02.2024.

Rad korigovan 23.05.2024.

Rad prihvaćen 3.06.2024